Pakistan J. Zool., pp 1-12, 2023. **DOI**: https://dx.doi.org/10.17582/journal.pjz/20230628050654

Preparation of High Selenized *Gastrodia elata* Blume Polysaccharide and its Immunomodulatory Effects on RAW264.7 Cells and Cyclophosphamide-Treated Mice

Fengwei Ma[1]*, Qihua Wen[1], Qingfang Deng[2], Yihao Lu[1], Buyan Zhang[1], Yongyou Cheng[1] and Su Xu[1]*

[1]College of Food Science and Engineering, Guiyang University, Guiyang 550005, China
[2]Key Laboratory for Information System of Mountainous Areas and Protection of Ecological Environment, Guizhou Normal University, Guiyang 550001, China

Fengwei Ma and Qihua Wen contributed equally to this work.

Article Information
Received 28 June 2023
Revised 25 August 2023
Accepted 23 September 2023
Available online 31 October 2023 (early access)

Authors' Contribution
Conceptualization and funding acquisition: FM and SX. Investigation: FM, QW and QD. Resources: YL, FM and SX. Formal analysis: FM, BZ. Software: FM and QW. Visualization: QD. Supervision: FM, YC and SX. Writing original draft: FM. Writing-review and editing: YC, SX. All authors contributed to the article and approved the submitted version.

Key words
***Gastrodia elata* Blume, Polysaccharide, Selenylation modification, Structure elucidation, Immunomodulatory activity**

ABSTRACT

Selenium (Se) is an essential trace element for human and animal nutrition, its supplementation holds great significant. In the study, *Gastrodia elata* polysaccharide (GEP) was extracted and further purified via DEAE-52 column chromatography. High selenized *Gastrodia elata* polysaccharide (Se-GEP) was obtained by presulfation prior to the selenylation modification process. The structures of GEP and Se-GEP were characterized using various chemical analysis techniques, including ultraviolet (UV), Fourier-transform infrared spectroscopy (FT-IR), nuclear magnetic resonance (NMR), scanning electron microscopy (SEM), energy dispersive X-ray (EDX), high-performance liquid chromatography (HPLC), high-performance gel permeation chromatography (HPGPC), periodate oxidation analysis. Their immunostimulatory activities were further investigated *in vitro* and *in vivo*. The results demonstrated the successful introduction of the seleninic group into GEP with substitution occurring at the C-6 position of glucose. The particle sizes decreased from 819.8 nm to 395.4 nm, and the absolute values of the zeta potential increased from 24.57 mV to 28.17 mV, indicating that selenylation modification improved GEP's physical stability. Se-GEP enhanced RAW264.7 cell proliferation, cell phagocytosis, and secretion of nitric oxide (NO) and interleukin (IL)-1β compared to the GEP group. Furthermore, Se-GEP improved the immunological activity by increasing spleen and thymus indices, enhancing phagocytic function, and activating both Th1 and Th2 lymphocytes. The findings provide valuable insights for the development of Se-GEP as dietary selenium nutrient supplements.

INTRODUCTION

Selenium (Se) is a vital trace element that is essential for both humans and animals (Lian *et al*., 2018). However, the natural abundance of Se is low. Therefore, it is necessary to develop Se-containing materials for various applications, including pharmacology and material sciences (Debnath *et al*., 2022). Selenylation of polysaccharides has been extensively adopted to develop novel sources of Se supplements and to improve the activity of polysaccharides (Cheng *et al*., 2018). Selenized polysaccharides have demonstrated noteworthy activities such as antioxidant, antitumor, antidiabetic, and immunomodulatory activities (Yuan *et al*., 2017; Wu *et al*., 2020; Zhang *et al*., 2021). The Se content in selenized polysaccharides has been shown to significantly influence their biological activities (Liu *et al*., 2021). For instance, higher Se content in selenized polysaccharides correlates positively with improved antitumor and antioxidant activities using selenized *Artemisia sphaerocephala* or selenized *Ulmus pumila* L. polysaccharides (Lee *et al*., 2017; Liu *et al*., 2021). Thus, optimizing the Se content is a critical factor in improving the biological potential of selenized polysaccharides.

Conventionally, nitric acid-sodium selenite (HNO_3-Na_2SeO_3, NA-SS) method has been used to prepare selenium-modified polysaccharides. However, this method

* Corresponding author: mfw200422501212@163.com, xs8515@126.com
0030-9923/2023/0001-0001 $ 9.00/0

often yields selenized polysaccharides with low Se content. Alternative selenylation techniques have been explored, such as glacial acetic acid-sodium selenite (GA-SS), glacial acetic acid-selenous acid (GA-SA), and selenium oxychloride (SOC), but the NA-SS reaction remains the most common method adopted (Cheng *et al*., 2018). It is reported the Se content of selenized *Grifola frondosa* polysaccharide was only 445.39 μg/g by direct using NA-SS method (Li *et al*., 2022). Similarly, even under optimal conditions, selenized *Artemisia sphaerocephala* polysaccharide achieved a high Se content (1703 μg/g) with the NA-SS method (Wang *et al*., 2012). To address this limitation, a new polysaccharide selenylation system needs to be developed to improve the effectiveness.

Selenium and sulfur are analogs in the same group VIA of the periodic table, and polysaccharides containing sulfur can be replaced by Se via a sulfation- and selenation-replacement reaction (Bi *et al*., 2018, 2020). Selenylation modification of sulfated polysaccharides, such as kappa-selenocarrageenan, has been well accomplished and widely used in food, medicine, agriculture and various other fields (Wang *et al*., 2013, 2021). Furthermore, the presence of selenate has been found to block the synthesis of heparan sulfate and chondroitin sulfate in cultured cells, which further validated the special relationship between selenium and sulfur (Dietrich *et al*., 1988). Therefore, pre-sulfation modification of sulfur-lacking polysaccharides prior to selenylation may offer a viable approach to improve the effectiveness in the preparation of selenized polysaccharides (Bi *et al*., 2018, 2020).

Gastrodia elata (*G. elata*) Blume, belonging to Orchidaceae family, is predominantly found in mountainous regions of eastern Asia, including China, India, etc. (Zhan *et al*., 2016). The rhizome of *G. elata* (commonly called 'Tian ma' in traditional Chinese medicine) has been recognized as a nutritious food source. Its major active ingredients were gastrodin, gastrodin aglycone (4-hydroxybenzyl alcohol) and *G. elata* polysaccharides (GEP) (Chen *et al*., 2012; Huo *et al*., 2021). The water-soluble polysaccharide components in *G. elata* constitute more than 10% of its dry weight and possess a variety of biological activities, such as antidepressant, angiotensin-I converting enzyme (ACE)-inhibitory, immunomodulatory, modulating gut microbiota, anti-ischemic stroke, and anti-aging activities (Lin *et al*., 2018; Zhu *et al*., 2019a, b; Guan *et al*., 2022; Huo *et al*., 2021; Li *et al*., 2016). The extensive pharmacological effects of GEPs show their great potential for pharmaceutical and food industry applications. However, to date, natural selenium polysaccharides in *G. elata* have not been reported.

In this study, in order to obtain selenized GEP with a high selenium content and investigate the immunomodulatory effects of selenium-modified GEP, GEP was extracted, purified and modified through selenylation after a pre-sulfation process. The immunoregulatory effects of selenized *G. elata* polysaccharides were evaluated *in vitro* using RAW264.7 cells and *in vivo* using cyclophosphamide-treated mice. By developing a highly selenized GEP and investigating its immunoregulatory effects, this research have implications for the development of novel dietary selenium nutrients for improving human immunity.

MATERIALS AND METHODS

Materials and reagents

The rhizomes of *Gastrodia elata* were from Guizhou Wumengteng Fungus Industry Co., Ltd. (Guizhou, China) and stored at College of Food Science and Engineering, Guiyang University (voucher specimen no. 2021002005). RAW264.7, a macrophage cell line, was from American Type Culture Collection (ATCC, Manassas, VA, USA). Main chemicals and reagents were listed in Table S1, all other reagents were of analytical grade and commercially available.

Extraction and purification of GEP

To extract GEP, dried *G. elata* rhizomes (506 g) were defatted thrice with 95% ethanol, and refluxed thrice with boiling water, following a modified methods (Li *et al*., 2023). The supernatant was concentrated to 1/4 of its initial volume, and treated with Sevag reagent (*v/v*, 2:1) to remove proteins. Ethanol was added to a final concentration of 80% and stored at 4°C for 24 h. After centrifugation, the precipitate was re-dissolved in distilled water and lyophilized to yield crude polysaccharides.

For purification, a diethylaminoethyl cellulose-52 (DEAE-52) ion exchange resin column (30 cm × 3.2 cm) was employed. The crude polysaccharides were eluted from column using deionized water at a flow rate of 1 mL/min, and collected at every 10 mL, the phenol-sulfuric acid method was employed to monitored the elution. The most abundant fraction of polysaccharides obtained from DEAE-52 was lyophilized, yielding purified GEP.

Preparation of sulfated GEP and selenized GEP

To prepare sulfated GEP, chlorosulfonic acid-pyridine (CSA-Pyr) method with modifications was used (Liu *et al*., 2015). Briefly, GEP (1 g) was suspended in N, N-dimethylformamide (DMF) and stirred for 1 h (25°C). The sulfated reagent was prepared by adding CSA to Pyr at a ratio of 1:2 (*v/v*) in an ice bath, and energetically stirred for 1 h (25°C). Then the sulfated reagent was added dropwise to the GEP and stirred for 2 h (25°C). After the

reaction was finished, the pH of the mixture was adjusted to 7 using NaOH (2 mol/L). After that, ethanol was added (3-fold volume) and kept at 4°C for 24 h to collect the precipitate. Then, redissolved, dialyzed against distilled water for 24 h using with MW cutoff of 3500 Da. Finally, lyophilized to obtain sulfated GEP.

The selenylation modification of sulfated GEP was conducted using a modified NA-SS method (Lian *et al*., 2018). Briefly, 500 mg of sulfated GEP was added to 100 mL of HNO_3 (0.3%, *v/v*) containing 1.0 g of $BaCl_2$ under full stirring. The selenylation reaction was initiated by adding 500 mg of Na_2SeO_3, with reaction for 4 h at 70°C. Subsequently, was cooled to room temperature, and adjusted pH to 7 using NaOH (1 mol/L). Sodium sulfate (Na_2SO_4) was added to remove Ba^{2+}, then centrifuged at 3500 rpm for 10 min. The resulting aqueous fraction was extensively dialyzed with water for 48 h and further with distilled water for 24 h, until no free sodium selenium was detected when ascorbic acid (Vc) was added. Finally, the dialysate was concentrated and lyophilized to obtain selenized polysaccharide (Se-GEP). The direct selenylation of GEP without prior sulfation was also performed using the same method.

Determination of selenium and sulfur contents

A fluorescence spectrophotometer (RF-5301PC, Shimadzu, Kyoto, Japan) was employed to determine the selenium content. First, 10 mg of Se-GEP or directly selenized GEP was added into 4 mL acid ($HClO_4$:H_2SO_4:HNO_3 = 1:1:4, *v/v/v*) and digested in a microwave digestion workstation using a preset program (room temperature to 80°C for 10 min, 80°C to 140°C for 5 min, 140°C to 210°C for 3 min, hold at 210°C for 15 min, and vent for 20 min). Subsequently, the digested sample was placed into a 100 mL conical flask and heated until almost dry. After cooling, the digestion solution was diluted to 10 mL with 0.1 mol/L HCl. Hydroxylamine hydrochloride ($HONH_2$·HCl, 0.5 mol/L, 4 mL) and ethylenediaminetetraacetic acid disodium (EDTA-2Na, 0.2 mol/L, 4 mL) were added. Next, 2 mL of 0.1% 2,3-diaminonaphthalene (DAN) was added, then kept in dark for 1 h. Subsequently, heated for 10 min in boiling water, cooled to room temperature, and added 5 mL of cyclohexane, with its fluorescence intensity measured with excitation and emission wavelengths of 376 nm and 520 nm, respectively. Finally, the Se content was calculated according to a standard curve. The sulfur content (S%) and the degree of substitution (DS) of GEP and its derivatives were measured using the barium chloride-gelatin method (Ji *et al*., 2013).

Physicochemical properties of GEP and its derivatives

Total sugar content of GEP and its derivatives was measured using phenol-sulfuric acid method with D-glucose as the standard (DuBois *et al*., 1956). Reducing sugar content was determined using the 3,5-dinitrosalicylic acid (DNS) with D-glucose as the standard (Wu *et al*., 2020). To measure protein content, the Bradford method was adopted with bovine serum albumin (BSA) as the standard (Bradford, 1976). The uronic acid content was determined using the carbazole-sulfuric acid method with D-galacturonic acid as the reference (Blumenkrantz and Asboe-Hansen, 1973).

Molecular weight was accessed using high-performance gel permeation chromatography (HPGPC, Agilent 1260 series) with a TSK gel G4000 SWXL column (7.8 mm × 300 mm) and a differential refractive detector (RID, G1362A). Polysaccharide samples (5 mg/mL in distilled water) were filtered (0.45 μm) and injected (10 μL). Isocratic elution with distilled water was conducted at a flow rate of 0.6 mL/min. T-series dextran was adopted as the calibrated standard for the MW measurement.

To estimate the stability of the polysaccharide dispersion system, polysaccharide samples were diluted with deionized water to a final concentration of 1.0 mg/mL. After centrifugation, average particle size and zeta potential (ZP) were determined at 25°C with a fixed scattering angle of 90° using a NanoZS90 zeta-sizer (Malvern, Worcestershire, UK).

Structural characterization of GEP and Se-GEP

The UV spectra of GEP and Se-GEP samples (0.1 mg/mL) were measured using a UV- spectrophotometer (UV2600, Shimadzu, Japan) in the range of 200–400 nm. The samples were prepared as KBr pellets and detected by a Fourier-transform infrared spectroscopy (FT-IR) spectrometer (iCan 9, Tianjin, China) in a wavenumber range of 400–4000 cm^{-1}. After complete acid hydrolysis and derivatization with 1-phenyl-3-methyl-5-pyrazolone (PMP), monosaccharide composition analysis of GEP was conducted by HPLC (Yang *et al*., 2005).

The microstructures of GEP and Se-GEP were observed under a scanning electron microscope (JSM-5510, JEOL, Tokyo, Japan) (Hanani *et al*., 2012). Prior to examination, the polysaccharides were coated with a thin layer gold film, and images were obtained (accelerating voltage of 2 kV). Surface elemental compositions of polysaccharides were measured using EDX spectroscopy (EX-250, Horiba Ltd., Tokyo, Japan).

Nuclear magnetic resonance (NMR) spectroscopy of Se-GEP was performed on a Bruker Avance NEO spectrometer (Bruker, Karlsruhe, Germany) operating at a frequency of 600 MHz with tetramethylsilane (TMS)

as the internal reference (Lou *et al*., 2022). Se-GEP was deuterium-exchanged by freeze-drying from D_2O and then dissolved in D_2O for examination using a 5-mm probe at room temperature.

The presence of branches in Se-GEP skeleton structure was investigated by examining the blue color in the iodine-starch reaction (Tuvaanjav *et al*., 2016). Briefly, polysaccharide (5.0 mL, 1.0 mg/mL) was placed in glass colorimetric tubes (25 mL), followed by adding 1.0 mL of iodine solution (0.2% KI containing 0.02% I_2). After vigorous shaking for 5 min, the color change was observed to determine the presence of branches in polysaccharide main chain and the presence of starch. To identify the triple-helix conformation of polysaccharides, the Congo red reaction assay was conducted by monitoring the shift in visible absorption maximum at different alkali concentrations (Yu *et al*., 2010). Se-GEP (0.5 mg/mL) in 0–0.5 mol/L NaOH containing 80 μmol/L Congo red were prepared, to measure the absorption (from 190 nm to 800 nm).

The Se substitution site was identified using periodate oxidation and formic acid formation tests. Each 1→6 pyranose residue with hydroxyl groups on three contiguous carbon atoms undergoes periodate oxidation and liberates one mole of formic acid (Kent, 1949). GEP and Se-GEP (50 mg) in 30 mmol/L $NaIO_4$ (25 mL) were kept in dark for 7 days at room temperature. The consumption of $NaIO_4$ and liberation of formic acid from GEP and Se-GEP were examined and compared.

In vitro *immunomodulatory activity analysis*

RAW264.7 cells, cultured in high-glucose DMEM with 10% (*v/v*) heat-inactivated fetal bovine serum (FBS) and 1% (*v/v*) penicillin-streptomycin (5000 units/mL penicillin, 5000 μg/mL streptomycin), were incubated in a humidified atmosphere of 5% CO_2 at 37°C (NUAIR-NU-5510E, USA). The cell viability assay of the polysaccharides was performed using a cell counting kit 8 (CCK-8, Solarbio; Beijing, China). Different dose levels (10, 20, 40, 60, and 80 μg/mL for GEP and Se-GEP) with 10 μg/mL polymyxin B were added to the treated wells for 12 and 24 h. LPS (500 ng/mL) was used as a positive control and PBS as a negative control. Similarly, cells were treated with Na_2SeO_3 (1, 2, 3, and 4 μg/mL). The absorbance were measured (450 nm) with Varioskan LUX microplate reader (Thermo Fisher, Waltham, MA, USA). Cell viability were calculated using absorbance of treatment group divided by that of the blank group, with the negative control cells designed with 100% viability.

The phagocytic activity was evaluated using neutral red method. Based on the cell viability test and preliminary experiments, samples at various dose levels (40, 80, 160, and 320 μg/mL for GEP and 5, 10, 15, and 20 μg/mL for Se-GEP) were added to the wells, with LPS (500 ng/mL) used as a positive control and PBS as a negative control. After incubation for 24 h, 100 μL of neutral red solution (1%) was added and incubated for 30 min. Then dumped the supernatant, and cells were washed with PBS (10 mmol/L, pH 7.2) for five times. Next, 200 μL of lysing buffer (ethanol:acetic acid = 1:1, *v/v*) was added and incubated for 2 h. The absorbance (at 540 nm) was measured, and the neutral red phagocytosis rate (%) was calculated using the absorbance of treatment group divided by that of the blank group.

RAW264.7 cells were seeded (1×10^5 cells/well). After 2 h of incubation, the cells were treated with samples (40, 80, 160, and 320 μg/mL for GEP; and 5, 10, 15, and 20 μg/mL for Se-GEP) in the presence and absence of LPS (1 μg/mL) for 24 h. The supernatants cells were collected, the amounts of tumor necrosis factor α (TNF-α) and nitric oxide (NO) production were detected using mouse TNF-α and NO ELISA kits.

In vivo *immunomodulatory activity analysis*

Male ICR mice (8 weeks old, 25–30 g), purchased from Chongqing Tengxin Biotechnology Co., Ltd. (license number: SCXK2019-0010), were housed with a 12 h light/dark cycle, 25 ± 1°C, and a humidity of 60 ± 10%. Before the experiments, the mice were acclimatized for 3 days and had free access to water and standard chow. They were randomly divided into 7 groups (n=10): sham (water), vehicle (cyclophosphamide 80 mg/kg/day), sodium selenite (Na_2SeO_3 30 μg/kg/day), positive control (lentinan, 50 mg/kg/day), low-, medium-, and high-dose Se-GEP (100, 500, and 3000 μg/kg/day) groups. Se-GEP doses based on the recommended humans intake (70 μg/day of Se), and converted to does in mice (Reagan-Shaw *et al*., 2008). The Se content in Se-GEP was calculated as 2.29%, so medium Se-GEP dose was fixed at 500 μg/kg/day, and low and high doses were determined through preliminary experiments. All groups, except the sham group, underwent immunosuppression by intraperitoneal administration of cyclophosphamide (80 mg/kg/day) for ten consecutive days. From day 11 to day 20, all groups received daily oral administration of respective polysaccharides or water. Body weight was measured on day 1, 10, and 20, and feed intake was recorded as the average value for days 1-10 and days 11-20. After the final administration, all mice were fasted for 24 h, mice were weighed and then sacrificed (cervical dislocation). The blood were collected, spleen and thymus tissues were weighed, and the relative organ indices were calculated.

The immune activity of macrophage cell function was assessed by a nonspecific carbon clearance test (Yang

et al., 2009). 0.1 mL/10 g of India ink (20%, *v/v*) were injected via the tail vein. Blood samples (20 μL) were collected from the retro-orbital venous plexus after 3 min (t_1) and 15 min (t_2) and immediately mixed with 2 mL of 0.1% sodium carbonate solution. The absorbance of these dilutions at 600 nm was measured, where OD1 for t_1 and OD2 for t_2. The phagocytic index (α) was calculated:

$$K = \frac{\log OD1 - \log OD2}{t_2 - t_1}$$

$$\alpha = \frac{Body\ weight}{Liver\ weight + Spleen\ weight} \times \sqrt[3]{K}$$

The serum was obtained by centrifuging the blood samples at 3500 rpm for 10 min at 4°C, and the levels of interleukin 4 (IL-4) and interferon gamma (IFN-γ) were measured using the respective ELISA kits, with lentinan (50 mg/kg/day) as a positive control.

Statistical analysis

All data are expressed as mean ± SD. One-way ANOVA was conducted for differences analysis with IBM SPSS 23.0 (Chicago, IL, USA) and GraphPad Prism 8.0 (La Jolla, CA, USA). Statistical significance was considered at P <0.05 and P <0.01.

RESULTS AND DISCUSSION

Physicochemical analysis

The efficient selenylation of GEP was achieved through the selenylation modification of sulfated GEP. The composition of GEP and its derivatives were listed in Table I, including total sugar, reducing sugar, protein, uronic acids, *etc*. The total sugar content in GEP was 93.18%. GEP contained no sulfur, but after presulfation, the sulfur content and DS of sulfated GEP were determined to be 7.16% and 0.47, respectively. Under the mentioned preparation conditions, a maximum Se content of 22,900 μg/g was observed in Se-GEP. Compared with direct selenylation of GEP (2805 μg/g) by the NA-SS method, it was obvious that selenylation efficiency was greatly improved with an approximately 8-fold higher Se content.

The average MWs of GEP and Se-GEP were estimated to be 524.4 and 488.9 kDa, respectively, using by the HPGPC method calibrated with a series of standard dextrans (Fig. 1A, B). Particle size distribution is an important physical parameter for nanoparticles, larger particle size tend to exhibit faster sedimentation rate with poor stability (Wu *et al.*, 2020). The average particle sizes of GEP and Se-GEP were 819.8 ± 124.6 and 395.4 ± 18.8 nm, respectively (Fig. 1C). These particle size results indicated that selenylation modification reduced the particle volume and improved physical stability. The zeta potential values confirmed that both GEP and Se-GEP exhibited electronegativity (Fig. 1D). The zeta potentials of GEP and Se-GEP were -24.57 ± 2.58 mV and -28.17 ± 1.59 mV, respectively. The higher absolute ZP value of Se-GEP compared to GEP is due to electronegative selenite ions.

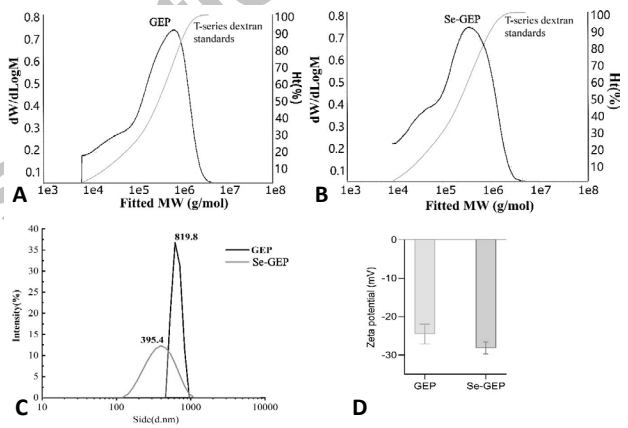

Fig. 1. Average MW (A, B), particle size distribution (C), and Zeta potential values (D) of GEP and Se-GEP.
MW, molecular weight; GEP, *Gastrodia elata* polysaccharide; Se-GEP, selenylation modification of sulfated GEP. The black lines in panels A and B represent good purity of polysaccharide, and the peaks were reflected in a corresponding MW in x-axis. The gray lines indicate the distribution plot of T-series dextran standards for establishing the MW range.

Table I. Chemical analysis of GEP and its modified products.

Sample	Total sugar content (%)	Protein content (%)	Reducing sugar content (%)	Uronic acid content (%)	Se content (μg/g)
GEP	93.18±0.84	1.1±0.03	0.5±0.24	4.7±0.3	-
Direct selenized GEP	84.28±1.03	1.2±0.06	2.4±0.55	6.6±0.1	2805±183.6
Sulfated GEP	87.74±1.58	1.3±0.08	2.8±0.18	4.8±0.9	-
Se-GEP	81.83±1.52	1.1±0.04	2.6±0.59	9.1±1.1	22,900±2056

Notes: data are presented as mean ± SD. GEP, *Gastrodia elata* polysaccharide; Se-GEP, selenylation modification of sulfated GEP; -, not detected.

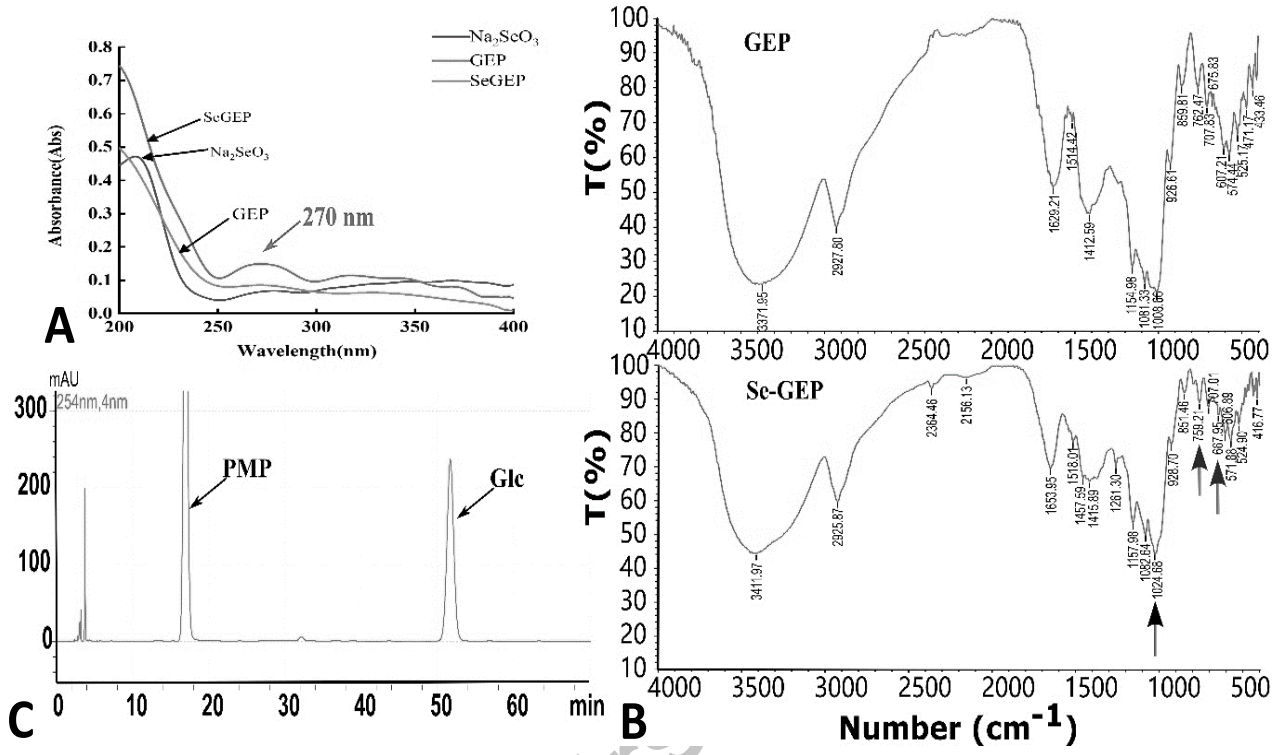

Fig. 2. (A) UV spectra of GEP and Se-GEP recorded from 200-400 nm, (B) FT-IR spectra of GEP and Se-GEP measured in the frequency range of 4000~400 cm^{-1}. (C) Chromatograms of monosaccharide composition analysis in GEP. UV, ultraviolet; FT-IR, Fourier-transform infrared spectra; PMP, 1-phenyl-3-methyl-5-pyrazolone; Glc, glucose. T (%), Transmittance (%).

Structural analysis of GEP and Se-GEP

The UV spectra of GEP and Se-GEP were recorded at a concentration of 0.1 mg/mL. GEP exhibited typical polysaccharide characteristics with no UV absorption at 200-400 nm, but by virtue of the selenite group, Se-GEP had a weak absorption at approximately 270 nm (Fig. 2A). The FT-IR spectra of GEP and Se-GEP exhibited several characteristic absorption peaks for a polysaccharide (Fig. 2B). There were two major bands: An absorption in the 3000-3600 cm^{-1} was associated with the O-H stretching vibration (Wang *et al*., 2014), and an absorption in the 1000-1400 cm^{-1} corresponded to the C-O-C stretching vibration (Yin *et al*., 2012). The absorptions at 1008.7, 1081.3 and 1155.0 cm^{-1} indicated the absence of the pyranose ring in the sugar residues (Zhang *et al*., 2021). In comparison to GEP, the absorption exhibited at 667.9 cm^{-1} (Se-O-C symmetrical stretching vibration), 759.2 cm^{-1} (stretching vibration of Se=O group), and 1024.7 cm^{-1} (O-Se-O bond in the selenium ester) (Wu *et al*., 2020). These results confirmed the successful preparation of Se-GEP. Monosaccharide composition analysis of GEP revealed that it mainly consisted of glucose (Fig. 2C).

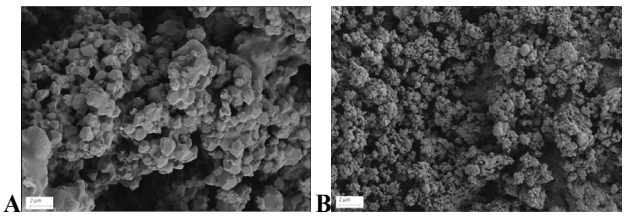

Fig. 3. Morphological characterization of GEP (A) and Se-GEP (B) under scanning electron (×1000).

The SEM results demonstrated that Se-GEP had a different microstructure compared to GEP. GEP exhibited isolated solid blocks with irregular shapes, while Se-GEP displayed a smaller block and a dispersed loose surface (Fig. 3A, B). These morphological changes suggested that the selenylation process might change the initial intact dense structure and lead to the formation of heterogeneous-sized blocks. EDX analysis indicated that both GEP and Se-GEP primarily consisted of carbon (C) and oxygen (O) elements, while in Se-GEP, characteristic absorption peaks of Se and S occurred in the EDX spectra (Supplementary Fig. S1A, B). The presence of the sulfur element signal in

Se-GEP might be due to the presulfation reaction before selenylation process.

The ^{1}H NMR spectrum of Se-GEP showed characteristic signals mainly from δ_H 3.06 to 5.28 ppm, while the ^{13}C NMR spectrum exhibited signals mainly in the range of δ_c 59.99 ppm to 103.59 ppm (Supplementary Fig. S2A, B), which are typical signals for polysaccharides (Guan *et al*., 2022). The ^{1}H NMR spectrum (Supplementary Fig. S2A) revealed signals in anomeric region at δ_H 5.28, δ_H 5.27, δ_H 5.09, δ_H 5.04, δ_H 4.84, and δ_H 4.50, indicating Se-GEP contains both α- and β-type configurations of sugars, which were mainly present in the α-configuration. The presence of H_2O or HDO attributed to a larger signal at δ 4.68.

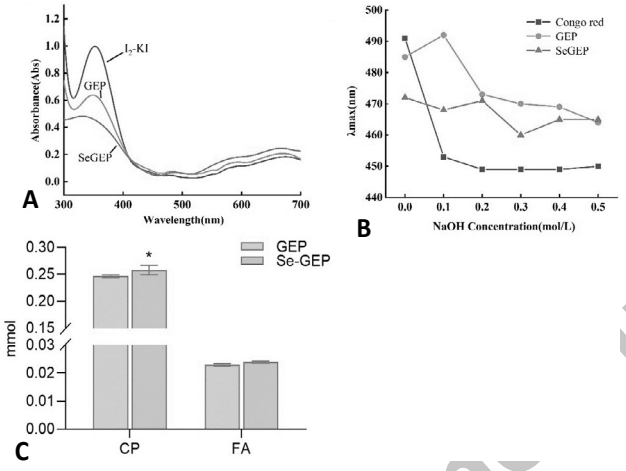

Fig. 4. The I_2-KI test of GEP and Se-GEP (A), the maximum absorption wavelength of Congo red test at various concentrations of NaOH (B), and the periodate consumption and formic acid formation of GEP and Se-GEP during periodate oxidation (C). CP, consumption of periodate, FA, formic acid formation.

The maximum absorption peaks of GEP and Se-GEP in the I_2-KI test were centered at approximately 350 nm, with no peaks observed at approximately 565 nm (Fig. 4A). This indicated that both GEP and Se-GEP had high molecular weights and contained numerous branched chains connected to the main structure (Guo *et al*., 2016). Furthermore, the lack of reaction of GEP and Se-GEP with the iodine reagent demonstrated the absence of starch in the structure. The interaction between Congo red and polysaccharides could, which exhibit a triple helical conformation, results in a shift towards longer wavelength in absorption. There were notable shifts in λ_{max} for GEP and Se-GEP with increasing NaOH concentration from 0-0.1 M and 0-0.2 M, respectively (Fig. 4B). However, a descending behavior of λ_{max} occurred at high NaOH concentrations (0.2-0.5 M), which is possibly due to the breakdown of hydrogen bonding or hydrophobic interactions between Se-GEP and Congo red (Pesek *et al*., 2022). These findings suggested that GEP and Se-GEP existed as both triple-helical and random coil structures.

Periodate oxidation is commonly used to elucidate the structures of carbohydrates due to its specificity for vicinal diols (Kristiansen *et al*., 2010). As shown in Figure 4C, the periodate oxidation of GEP and Se-GEP produced 0.0229 mmol and 0.0239 mmol of formic acid (FA), respectively, indicating the presence of 1→6 linkage or 1→ linkage terminal saccharide residues. Additionally, 0.246 mmol and 0.258 mmol of periodate were consumed, respectively. The consumption of periodate was more than two times that of FA production, indicating the presence of 1→4 or 1→4,6 linkages. The existence of a 1→3 linkage in GEP and Se-GEP was also indicated by the fact that less than one mole of periodate was consumed per mole of glucose residue.

In vitro *effects of Se-GEP on RAW264.7 macrophages*

Macrophages are one of the most important immune cells and their activation has been considered to be a necessary step for immune system stimulation. The cell viability of RAW264.7 cells was examined by CCK-8 assay, with LPS as a positive control and PBS as a negative control. RAW264.7 cells exposed to GEP or Se-GEP samples at concentrations of 10-80 μg/mL for 12 h showed increased cell viability. The cells obtained growth promotion dose-dependently for GEP, and the cell viability reached a maximum of 122.1% ± 3.5% at 80 μg/mL (Fig. 5A). However, Se-GEP group exhibited a maximum cell viability reached of 147.8% ± 10.4% at 20 μg/mL for 12 h, which was almost equal to the LPS group (150.1% ± 9.5%). Meanwhile, Se-GEP promoted cell growth more effectively than GEP, especially at doses of 10 and 20 μg/mL, confirming that chemical selenylation enhanced the bioactivity of GEP. However, after incubation for 24 h, the high dose Se-GEP group (especially at 80 μg/mL) exhibited reduced cell viability, possibly due to selenium toxicity (Fig. 5B). When RAW264.7 cells were treated with Na_2SeO_3 alone at 1-4 μg/mL for 12-24 h, it mostly exerted cytotoxic effects on the cells (Fig. 5C). When the treatment time was 12 h, the high-dose Na_2SeO_3 group (4 μg/mL) resulted in a reduction in cell viability to 75.1%. When the treatment time was 24 h, higher concentrations of Na_2SeO_3 (3 and 4 μg/mL) caused significant cell death. These results indicate that inorganic Se (i.e., the Na_2SeO_3 form) is highly toxic when overdosed.

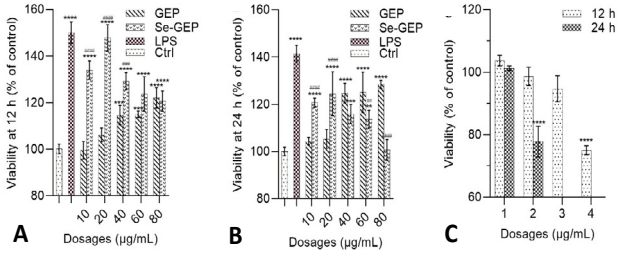

Fig. 5. The viability of RAW264.7 cells exposed to GEP, Se-GEP or Na_2SeO_3.
Notes: (A, B) Exposure for 12 h (A) and 24 h (B). (C) Exposure to Na_2SeO_3 for 12 h and 24 h. The data are presented as mean ± SD. ** $P < 0.01$, *** $P < 0.001$, and **** $P < 0.0001$, compared with the negative control group. $^{\#\#}$ $P < 0.01$, $^{\#\#\#}$ $P < 0.001$, and $^{\#\#\#\#}$ $P < 0.0001$ compared between the GEP and Se-GEP groups. Ctrl, blank, negative control; LPS, Lipopolysaccharide, positive control; GEP, *Gastrodia elata* polysaccharide; Se-GEP, selenylation of sulfated GEP.

To further assess the immune-regulatory potential of GEP and Se-GEP, doses of 40, 80, 160, and 320 μg/mL for GEP and 5, 10, 15, and 20 μg/mL for Se-GEP, were selected for subsequent cell experiments. When RAW264.7 cells were stimulated with GEP and Se-GEP at different concentrations for 24 h, their phagocytosis activity increased in a dose-dependent manner (Fig. 6A). Compared to GEP, Se-GEP exhibited stronger potential in enhancing macrophage phagocytosis at lower concentrations (from 107.4% to 120.5%). Additionally, GEP alone enhanced macrophage phagocytosis at higher doses of 160 and 320 μg/mL, resulting in phagocytosis values of 109.0% and 112.9%, respectively (Fig. 6A). These findings demonstrated that chemical selenylation of GEP promotes RAW264.7 cell phagocytosis.

TNF-α and NO are important mediators in the immune system. The secretion of TNF-α and NO from RAW264.7 cells was determined. GEP groups induced a dose-dependent increase in the secretion of NO and TNF-α in comparison with the blank control group. Similar results were observed for the Se-GEP group at doses of 5-20 μg/mL. Specifically, exposure of RAW264.7 cells to Se-GEP resulted in increased TNF-α secretion levels ranging from 407.4 to 490.5 pg/mL, and NO secretion levels elevated to 17.4-35.8 μM, compared to the control group (228 pg/mL TNF-α and 5.1 μM NO). Similarly, the GEP group at different dosages also exhibited elevated secretion levels of NO and TNF-α, but Se-GEP demonstrated a greater potential than GEP in promoting the secretion of these two cytokines (Fig. 6B, C). These results indicate that selenylation modification enhances the immunomodulatory activity of GEP.

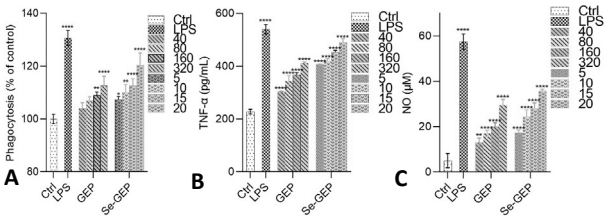

Fig. 6. Phagocytosis activity analysis (A) and secretion levels of TNF-α (B) and NO (C) of RAW264.7 cells exposed to GEP and Se-GEP at different dosages for 24 h.
Notes: Ctrl, blank, negative control; LPS, lipopolysaccharide, 500 ng/mL, positive control; GEP at doses of 40, 80, 160, and 320 μg/mL; Se-GEP at doses of 5, 10, 15, and 20 μg/mL, respectively. TNF-α, tumor necrosis factor α; NO, nitric oxide. The data are presented as mean ± SD. * $P < 0.05$, ** $P < 0.01$, and **** $P < 0.0001$, compared with the negative control group.

In vivo *effects of Se-GEP on cyclophosphamide (CTX)-treated mice*

The body weights and feed intake data are shown in Table II. Initially, the data did not differ significantly among all 7 groups. Compared with the sham group, all cyclophosphamide-treated mice groups exhibited significant decreases in body weight (P <0.0001) and feed intake (P <0.0001), indicating successful establishment of the immunosuppression model. After 10 days, all groups except the sham and vehicle groups received the respective polysaccharide treatments. The Se-GEP group showed significantly increased average body weights compared to the vehicle group, indicating that Se-GEP effectively improved immunomodulatory activity.

The vehicle group exhibited markedly decreased indices of spleen and thymus, compared to the sham group (P <0.0001), indicating immunosuppressive effects of cyclophosphamide. Treatment with Se-GEP demonstrated a dose-dependent increase in the spleen and thymus indices, compared to the vehicle group (Fig. 7A). The addition of Se to GEP exhibited great immunomodulatory effects and reversed the immune organs atrophy induced by CTX.

To evaluate the phagocytic function, the carbon clearance assay was employed, with faster removal of carbon particles indicating enhanced phagocytic function. As shown in Figure 7B, the vehicle group exhibited a remarkable decrease in phagocytic index (α), compared to sham group (P <0.0001). Se-GEP effectively increased the phagocytic index (α) in a dose-dependent manner. Particularly at a dose of 3000 μg/kg/day, the phagocytic activity was restored from 3.57 to 4.58, approaching the index of the sham group (4.54). These results demonstrated that Se-GEP can enhance macrophage function in CTX-treated mice.

Table II. Changes in body weight and feed intake during mice experiment.

Treatment groups	Body weight (g)			Feed intake (g)	
	Day 1	Day 10	Day 20	Modeling phase	Recovery phase
Sham	22.3±1.02	25.3±2.13	30.5±1.42	15.7±1.13	21.0±1.61
Vehicle	22.4±1.04	20.8±2.11****	24.0±1.55****	8.0±1.05****	8.7±1.52$^{****\#\#\#\#}$
Positive	22.1±0.98	21.3±1.98****	28.0±1.98$^{*\#\#\#\#}$	8.4±0.95****	15.8±1.12$^{****\#\#\#\#}$
Na_2SeO_3	21.8±1.05	21.1±2.15****	26.7±1.95$^{****\#\#}$	8.1±1.18****	13.9±1.32$^{****\#\#\#\#}$
Low-dose Se-GEP	22.3±1.01	20.4±2.02****	26.8±1.71$^{****\#\#}$	7.8±1.21****	15.1±1.81$^{****\#\#\#\#}$
Medium-dose Se-GEP	22.1±0.99	21.0±1.86****	28.2±1.99$^{*\#\#\#\#}$	8.4±1.95****	16.2±0.92$^{****\#\#\#\#}$
High-dose Se-GEP	22.0±0.89	20.4±1.85****	29.2±1.89$^{\#\#\#\#}$	8.4±0.89****	18.9±1.74$^{\#\#\#\#}$

Notes: data are presented as mean ± SD (n = 10). * $P < 0.05$, and **** $P < 0.0001$, compared with the Sham control group. $^{\#\#}$ $P < 0.01$, and $^{\#\#\#\#}$ $P < 0.0001$, compared with the vehicle group.

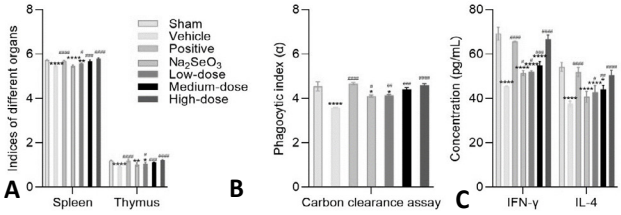

Fig. 7. Effects of Se-GEP on spleen and thymus indexes (A), carbon clearance assay (B) and the level of serum IFN-γ and IL-4 (C).
Notes: IFN-γ, interferon gamma; IL-4, interleukin 4. Data are presented as mean ± SD. * $P < 0.05$, ** $P < 0.01$, and **** $P < 0.0001$, compared with the Sham control group. $^{\#}$ $P < 0.05$, $^{\#\#}$ $P < 0.01$, $^{\#\#\#}$ $P < 0.001$, and $^{\#\#\#\#}$ $P < 0.0001$, compared with the vehicle group.

Activated T-helper type (Th1) and T-helper type (Th2) lymphocytes secrete IFN-γ and IL-4, respectively, which mediate cellular and humoral immune responses. Therefore, the levels of serum IFN-γ and IL-4 serve as indicators of cellular and humoral immunity. ELISA kits were used to determine the levels of serum IFN-γ and IL-4 with lentinan (50 mg/kg/day) as a positive control. The vehicle group exhibited a significant decrease in IFN-γ and IL-4 levels (Fig. 7C), indicating successfully CTX-induced immunosuppression in mice. While, treatment of Se-GEP led to a dose-dependent increase in IFN-γ and IL-4 levels, suggesting selenylation modification of GEP could enhance cellular as well as humoral immune in CTX-treated mice.

CONCLUSIONS

In this study, a highly selenized *Gastrodia elata* Blume polysaccharide (Se-GEP) was prepared through presulfation prior to selenylation modification. Se-GEP exhibited a molecular weight of approximately 500 kDa, with Se content of 2.29%, an average particle size of 395.4 ± 18.8 nm, and a zeta potential of -28.17 ± 1.59 mV. Structural analysis revealed that Se-GEP predominantly consists of glucose in the α-configuration and exists as both triple-helical and random coil conditions, where the selenylation reaction mostly occurs at the C-6 position. The immunomodulatory effects of Se-GEP on RAW264.7 cells demonstrated that Se-GEP treatment enhanced cell viability and phagocytosis and increased the secretion levels of NO and TNF-α. *In vivo* experiment of Se-GEP on CTX-treated mice revealed that administration of Se-GEP resulted in improved body weight and feed intake in immunosuppressive mice, increased the spleen and thymus indices, enhanced phagocytic function, and activated both Th1 and Th2 lymphocytes. Taken together, these findings suggested that Se-GEP holds potential as a dietary selenium nutrient for enhancing human immunity.

ACKNOWLEDGEMENTS

The exceptional contribution to authenticate Gastrodia elata by Prof, Huaguo Chen from Guizhou Normal University is greatly appreciated.

Funding

This research was supported by Guizhou Provincial Science and Technology Projects (Qian Ke He Pingtai Rencai-CXTD [2022]002, Qian Ke He JiChu [2019]1013), Guizhou Provincial Education Department (Qian Jiao Ji [2023]042), The special funding of Guiyang science and technology bureau and Guiyang University (GYU-KY [2021], GYU-KYZ [2018]-01-16, GYU-KYZ [2018]-01-20), Talent Introduction Program of Guiyang University (GYU-ZRD [2018]-022), and Young and middle-aged academic backbone of Guiyang University (GYURC-20).

Ethical approval

The protocols for the animal studies were approved by the Ethics Committee of the Institute of Laboratory Animal Resources of Guizhou Normal University (Guizhou, China, protocol code 2020030024).

Supplementary material

There is supplementary material associated with this article. Access the material online at: https://dx.doi.org/10.17582/journal.pjz/20230628050654

Statement of conflict of interest

The authors have declared no conflict of interest.

REFERENCES

Bi, D., Lai, Q., Cai, N., Li, T., Zhang, Y., Han, Q., Peng, Y., Xu, H., Lu, J. and Bao, W., 2018. Elucidation of the molecular-mechanisms and *in vivo* evaluation of the anti-inflammatory effect of alginate-derived seleno-polymannuronate. *J. Agric. Fd. Chem.*, **66**: 2083-2091. https://doi.org/10.1021/acs.jafc.7b05719

Bi, D., Li, X., Li, T., Li, X., Lin, Z., Yao, L., Li, H., Xu, H., Hu, Z. and Zhang, Z., 2020. Characterization and neuroprotection potential of seleno-polymannuronate. *Front. Pharmacol.*, **11**: 21. https://doi.org/10.3389/fphar.2020.00021

Blumenkrantz, N., and Asboe-Hansen, G., 1973. New method for quantitative determination of uronic acids. *Anal. Biochem.*, **54**: 484-489. https://doi.org/10.1016/0003-2697(73)90377-1

Bradford, M.M., 1976. A rapid and sensitive method for the quantitation of microgram quantities of protein utilizing the principle of protein-dye binding. *Anal. Biochem.*, **72**: 248-254. https://doi.org/10.1016/0003-2697(76)90527-3

Chen, X., Xiao, F., Wang, Y., Fang, J., and Ding, K., 2012. Structure-activity relationship study of WSS25 derivatives with anti-angiogenesis effects. *Glycoconjugate J.*, **29**: 389-398. https://doi.org/10.1007/s10719-012-9424-z

Cheng, L., Wang, Y., He, X. and Wei, X., 2018. Preparation, structural characterization and bioactivities of Se-containing polysaccharide: A review. *Int. J. Biol. Macromol.*, **120**: 82-92. https://doi.org/10.1016/j.ijbiomac.2018.07.106

Debnath, S., Agarwal, A., Kumar, N.R. and Bedi, A., 2022. Selenium-based drug development for antioxidant and anticancer activity. *Future Pharmacol.*, **2**: 595-607. https://doi.org/10.3390/futurepharmacol2040036

Dietrich, C.P., Nader, H.B., Buonassisi, V. and Colburn, P., 1988. Inhibition of synthesis of heparan sulfate by selenate: Possible dependence on sulfation for chain polymerization. *FASEB J.*, **2**: 56-59. https://doi.org/10.1096/fasebj.2.1.2961646

DuBois, M., Gilles, K.A., Hamilton, J.K., Rebers, P.A. and Smith, F., 1956. Colorimetric method for determination of sugars and related substances. *Anal. Chem.*, **28**: 350-356. https://doi.org/10.1021/ac60111a017

Guan, H., Ling, X., Xu, J., Zhu, Y., Zhang, J. and Liu, X., 2022. Structural characterization of polysaccharide derived from *Gastrodia elata* and its immunostimulatory effect on RAW264.7 cells. *Molecules*, **27**: 8059. https://doi.org/10.3390/molecules27228059

Guo, R., Ai, L., Cao, N., Ma, J., Wu, Y., Wu, J. and Sun, X., 2016. Physicochemical properties and structural characterization of a galactomannan from *Sophora alopecuroides* L. seeds. *Carbohydr. Polym.*, **140**: 451-460. https://doi.org/10.1016/j.carbpol.2015.12.058

Hanani, Z.N., Beatty, E., Roos, Y., Morris, M. and Kerry, J., 2012. Manufacture and characterization of gelatin films derived from beef, pork and fish sources using twin screw extrusion. *J. Fd. Eng.*, **113**: 606-614. https://doi.org/10.1016/j.jfoodeng.2012.07.002

Huo, J., Lei, M., Li, F., Hou, J., Zhang, Z., Long, H., Zhong, X., Liu, Y., Xie, C. and Wu, W., 2021. Structural characterization of a polysaccharide from *Gastrodia elata* and its bioactivity on gut microbiota, *Molecules*, **26**: 4443. https://doi.org/10.3390/molecules26154443

Ji, C.F., Ji, Y.B. and Meng, D.Y., 2013. Sulfated modification and anti-tumor activity of laminarin. *Exp. Ther. Med.*, **6**: 1259-1264. https://doi.org/10.3892/etm.2013.1277

Kent, P.W., 1949. Periodate oxidation in the study of the structure of dextrans. *Science*, **110**: 689-690. https://doi.org/10.1126/science.110.2869.689

Kristiansen, K.A., Potthast, A. and Christensen, B.E., 2010. Periodate oxidation of polysaccharides for modification of chemical and physical properties. *Carbohydr. Res.*, **345**: 1264-1271. https://doi.org/10.1016/j.carres.2010.02.011

Lee, J.H., Lee, Y.K. and Chang, Y.H., 2017. Effects of selenylation modification on structural and antioxidant properties of pectic polysaccharides extracted from *Ulmus pumila* L. *Int. J. Biol. Macromol.*, **104**: 1124-1132. https://doi.org/10.1016/j.ijbiomac.2017.06.121

Li, H.B., Wu, F., Miao, H.C. and Xiong, K.R., 2016.

Effects of polysaccharide of *Gastrodia elata* Blume and electro-acupuncture on expressions of brain-derived neurotrophic factor and stem cell factor protein in caudate putamen of focal cerebral ischemia rats. *Med. Sci. Monit. Basic Res.*, **22**: 175-180. https://doi.org/10.12659/MSMBR.901524

Li, N., Wang, D., Wen, X., Chu, R., Fan, J., Chen, Y. and Luo, Y., 2023. Effects of polysaccharides from *Gastrodia elata* on the immunomodulatory activity and gut microbiota regulation in cyclophosphamide-treated mice. *J. Sci. Fd. Agric.*, **103**: 3390-3401. https://doi.org/10.1002/jsfa.12491

Li, Q., Zhu, L., Qi, X., Zhou, T., Li, Y., Cai, M., Yan, Y., Qian, J.Y. and Peng, D., 2022. Immunostimulatory and antioxidant activities of the selenized polysaccharide from edible *Grifola frondosa*. *Fd. Sci. Nutr.*, **10**: 1289-1298. https://doi.org/10.1002/fsn3.2764

Lian, K.X., Zhu, X.Q., Chen, J., Liu, G. and Gu, X.L., 2018. Selenylation modification: Enhancement of the antioxidant activity of a *Glycyrrhiza uralensis* polysaccharide. *Glycoconjugate J.*, **35**: 243-253. https://doi.org/10.1007/s10719-018-9817-8

Lin, Y.E., Chou, S.T., Lin, S.H., Lu, K.H., Panyod, S., Lai, Y.S., Ho, C.T. and Sheen, L.Y., 2018. Antidepressant-like effects of water extract of *Gastrodia elata* Blume on neurotrophic regulation in a chronic social defeat stress model. *J. Ethnopharmacol.*, **215**: 132-139. https://doi.org/10.1016/j.jep.2017.12.044

Liu, C., Chen, J., Li, E., Fan, Q., Wang, D., Li, P., Li, X., Chen, X., Qiu, S., Gao, Z., Li, H. and Hu, Y., 2015. The comparison of antioxidative and hepatoprotective activities of *Codonopsis pilosula* polysaccharide (CP) and sulfated CP. *Int. Immunopharmacol.*, **24**: 299-305. https://doi.org/10.1016/j.intimp.2014.12.023

Liu, S., Hu, J., Li, M., Zhu, S., Guo, S., Guo, H., Wang, T., Zhang, Y., Zhang, J. and Wang, J., 2021. The role of Se content in improving anti-tumor activities and its potential mechanism for selenized *Artemisia sphaerocephala* polysaccharides. *Fd. Funct.*, **12**: 2058-2074. https://doi.org/10.1039/D0FO03013A

Lou, H.Y., Yi, P., Liu, H.F., Wang, H., Fu, J., Li, J.Y., Yang, Q.P., Zhang, S.L., Hao, X.J. and Pan, W.D., 2022. Novel flavonolignans from the roots of Indigofera stachyodes. *Fitoterapia*, **160**: 105217. https://doi.org/10.1016/j.fitote.2022.105217

Pesek, S., Lehene, M., Brânzanic, A.M.V. and Silaghi-Dumitrescu, R., 2022. On the origin of the blue color in the iodine/iodide/starch supramolecular complex. *Molecules*, **27**: 8974. https://doi.org/10.3390/molecules27248974

Reagan-Shaw, S., Nihal, M. and Ahmad, N., 2008. Dose translation from animal to human studies revisited. *FASEB J.*, **22**: 659-661. https://doi.org/10.1096/fj.07-9574LSF

Tuvaanjav, S., Shuqin, H., Komata, M., Ma, C., Kanamoto, T., Nakashima, H. and Yoshida, T., 2016. Isolation and antiviral activity of water-soluble *Cynomorium songaricum* Rupr. polysaccharides. *J. Asian Nat. Prod. Res.*, **18**: 159-171. https://doi.org/10.1080/10286020.2015.1082547

Wang, J., Yu, S., Jiao, S., Lv, X., Ma, M. and Du, Y., 2013. κ-selenocarrageenan prevents microcystin-LR-induced hepatotoxicity in BALB/c mice. *Fd. Chem. Toxicol.*, **59**: 303-310. https://doi.org/10.1016/j.fct.2013.06.022

Wang, J., Zhao, B., Wang, X., Yao, J. and Zhang, J., 2012. Synthesis of selenium-containing polysaccharides and evaluation of antioxidant activity *in vitro*. *Int. J. Biol. Macromol.*, **51**: 987-991. https://doi.org/10.1016/j.ijbiomac.2012.08.011

Wang, K., Liu, L., He, Y., Qu, C. and Miao, J., 2021. Effects of dietary supplementation with κ-selenocarrageenan on the selenium accumulation and intestinal microbiota of the sea cucumbers *Apostichopus japonicus*. *Biol. Trace Elem. Res.*, **199**: 2753-2763. https://doi.org/10.1007/s12011-020-02393-4

Wang, P., Liao, W., Fang, J., Liu, Q., Yao, J., Hu, M. and Ding, K., 2014. A glucan isolated from flowers of *Lonicera japonica* Thunb. Inhibits aggregation and neurotoxicity of Aβ42. *Carbohydr. Polym.*, **110**: 142-147. https://doi.org/10.1016/j.carbpol.2014.03.060

Wu, C., Zhao, M., Bu, X., Qing, Z., Wang, L., Xu, Y., Yang, Y. and Bai, J., 2020. Preparation, characterization, antioxidant and antiglycation activities of selenized polysaccharides from blackcurrant. *RSC Adv.*, **10**: 32616-32627. https://doi.org/10.1039/D0RA06462A

Yang, X., Zhao, Y., Wang, Q., Wang, H. and Mei, Q., 2005. Analysis of the monosaccharide components in *Angelica* polysaccharides by high performance liquid chromatography. *Anal. Sci.*, **21**: 1177-1180. https://doi.org/10.2116/analsci.21.1177

Yang, X.M., Yu, W., Ou, Z.P., Ma, H.L., Liu, W.M. and Ji, X.L., 2009. Antioxidant and immunity activity of water extract and crude polysaccharide from *Ficus carica* L. fruit. *Pl. Fds. Hum. Nutr.*, **64**: 167-173. https://doi.org/10.1007/s11130-009-0120-5

Yin, J., Chan, B.C., Yu, H., Lau, I.Y., Han, X., Cheng, S., Wong, C., Lau, C.B., Xie, M., Fung,

K., Leung, P. and Han, Q., 2012. Separation, structure characterization, conformation and immunomodulating effect of a hyperbranched heteroglycan from *Radix astragali*. *Carbohydr. Polym.*, **87**: 667-675. https://doi.org/10.1016/j.carbpol.2011.08.045

Yu, Z., Ming, G., Wang, K., Chen, Z., Dai, L., Liu, J. and Fang, Z., 2010. Structure, chain conformation and antitumor activity of a novel polysaccharide from *Lentinus edodes*. *Fitoterapia*, **81**: 1163-1170. https://doi.org/10.1016/j.fitote.2010.07.019

Yuan, B., Yang, X.Q., Kou, M., Lu, C.Y., Wang, Y.Y., Peng, J., Chen, P. and Jiang, J.H., 2017. Selenylation of polysaccharide from the sweet potato and evaluation of antioxidant, antitumor, and antidiabetic activities. *J. Agric. Fd. Chem.*, **65**: 605-617. https://doi.org/10.1021/acs.jafc.6b04788

Zhan, H.D., Zhou, H.Y., Sui, Y.P., Du, X.L., Wang, W.H., Dai, L., Sui, F., Huo, H.R. and Jiang, T.L., 2016. The rhizome of *Gastrodia elata* Blume. An ethnopharmacological review. *J. Ethnopharmacol.*, **189**: 361-385. https://doi.org/10.1016/j.jep.2016.06.057

Zhang, S., Zhang, H., Shi, L., Li, Y., Tuerhong, M., Abudukeremu, M., Cui, J., Li, Y., Jin, D.Q., Xu, J. and Guo, Y., 2021. Structure features, selenylation modification, and improved anti-tumor activity of a polysaccharide from *Eriobotrya japonica*. *Carbohydr. Polym.*, **273**: 118496. https://doi.org/10.1016/j.carbpol.2021.118496

Zhu, H., Liu, C., Hou, J., Long, H., Wang, B., Guo, D.A., Lei, M. and Wu, W., 2019a. *Gastrodia elata* Blume polysaccharides: A review of their acquisition, analysis, modification, and pharmacological activities. *Molecules*, **24**: 2436. https://doi.org/10.3390/molecules24132436

Zhu, Z.Y., Chen, C.J., Sun, H.Q. and Chen, L.J., 2019b. Structural characterisation and ACE-inhibitory activities of polysaccharide from Gastrodia elata Blume. *Nat. Prod. Res.*, **33**: 1721-1726. https://doi.org/10.1080/14786419.2018.1434643

Pakistan J. Zool., pp 1-12, 2023. **DOI**: https://dx.doi.org/10.17582/journal.pjz/20230628050654

Supplementary Material

Preparation of High Selenized *Gastrodia elata* Blume Polysaccharide and its Immunomodulatory Effects on RAW264.7 Cells and Cyclophosphamide-Treated Mice

Fengwei Ma[1]*, Qihua Wen[1], Qingfang Deng[2], Yihao Lu[1], Buyan Zhang[1], Yongyou Cheng[1] and Su Xu[1]*

[1]College of Food Science and Engineering, Guiyang University, Guiyang 550005, China
[2]Key Laboratory for Information System of Mountainous Areas and Protection of Ecological Environment, Guizhou Normal University, Guiyang 550001, China

Fengwei Ma and Qihua Wen contributed equally to this work.

Supplementary Table SI. Reagents and chemicals in this study.

Chemical and reagent	Producer or vendor
Dimethyl sulfoxide (DMSO), Trifluoroacetic acid (TFA), Nitric acid (HNO_3), sodium selenite (Na_2SeO_3), chlorosulfonic acid ($ClHSO_3$), pyridine, 1-phenyl-3-methyl-5-pyrazolone (PMP)	Aladdin (Shanghai, China)
T-series dextran standards (T-410, T-270, T-150, T-70, T-40, and T-10)	Sigma-Aldrich (St. Louis, MO, USA)
Dialysis tubes (MW 3500 Da)	Viskase (Lombard, IL, USA)
Lipopolysaccharide (LPS, from *Escherichia coli* 0111:B4), 2-(2-Methoxy-4-nitrophenyl)-3-(4-nitrophenyl)-5-(2,4-disulfophenyl)-2H-tetrazolium sodium (WST-8)	Solaibao Biotech (Beijing, China)
Nitric oxide (NO), mouse ELISA kits	Sigma Chemical (St. Louis, MO, USA)

* Corresponding author: mfw200422501212@163.com, xs8515@126.com
0030-9923/2023/0001-0001 $ 9.00/0

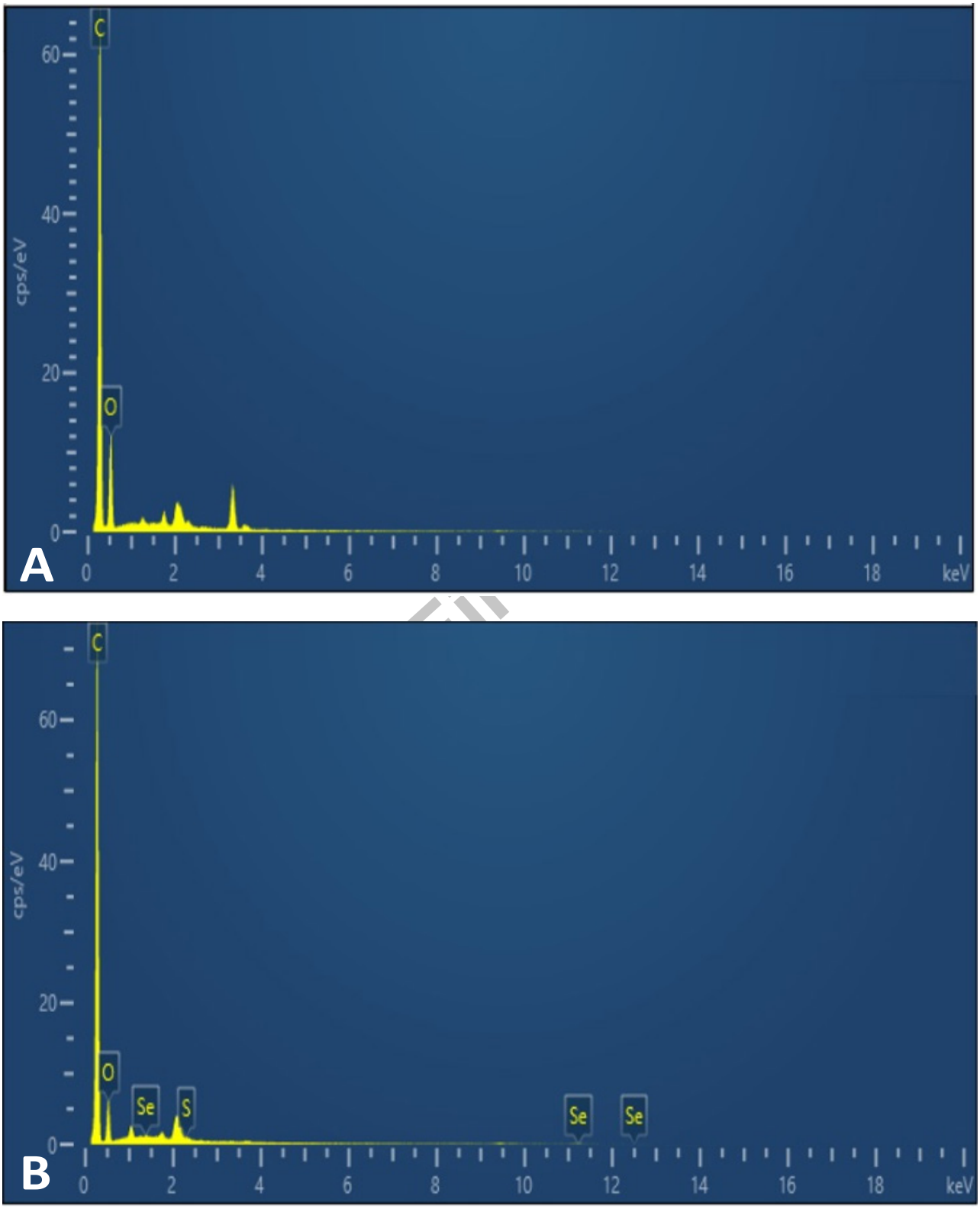

Supplementary Fig. S1. Surface elemental compositions of GEP (A) and Se-GEP (B).

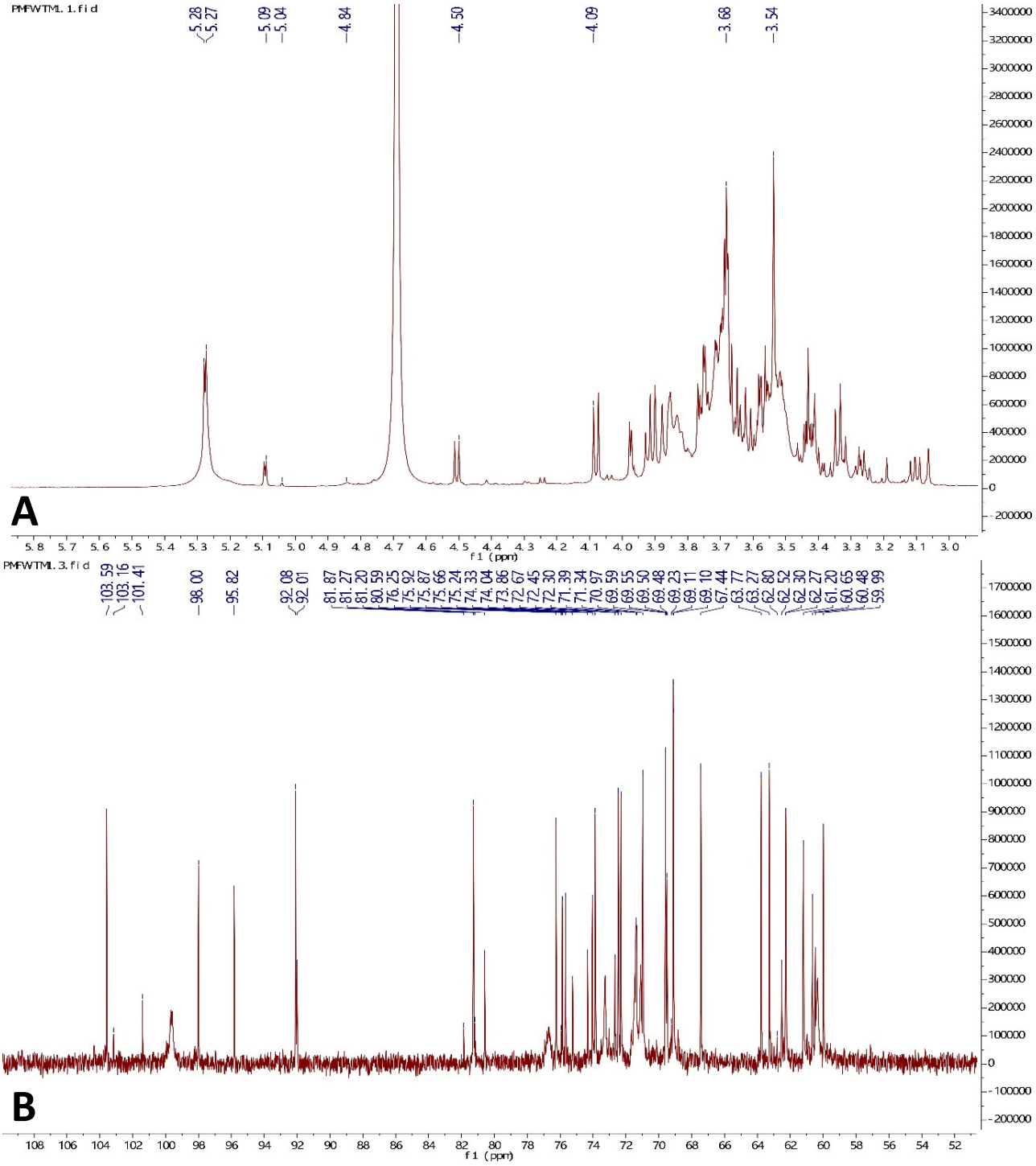

Supplementary Fig. S2. The NMR spectra of Se-GEP measured in a 5-mm NMR tube with 0.5 mL of 99.9% D_2O, (A) ^{1}H NMR; (B) ^{13}C NMR.